PASJ: Publ. Astron. Soc. Japan **47**, 429–437 (1995)

Accretion Disks Driven by External Radiation Drag around Central Luminous Sources

Jun FUKUE
Astronomical Institute, Osaka Kyoiku University, Asahigaoka, Kashiwara, Osaka 582
and
Masayuki UMEMURA
Institute of Physics, The University of Tsukuba, Tsukuba, Ibaraki 305

(Received 1994 November 15; accepted 1995 April 24)

Abstract

Accretion disks/disk accretions (*β-disks*) driven by the external radiation drag exerted by a central luminous source are presented under the steady and subrelativistic approximations. In a cold regime, where the gravity of the central object, the radiation force, and the radiation drag are included, but the pressure-gradient force is neglected, we find steady solutions such that the infalling velocity v_r is inversely proportional to radius r far from the center and becomes constant near to the center, while the rotation velocity v_φ is Keplerian far from the center and drops exponentially near to the center. In a warm regime, where the effect of the gas pressure is also taken into account, we find steady transonic solutions such that a flow accreting subsonically and rotating with the Keplerian velocity far from the center becomes, after passing a sonic point, an almost radially accreting supersonic flow with no angular momentum. Due to the effect of external radiation drag, the angular momentum of the gas is removed. In particular, it is quickly lost inside the characteristic radius r_0, which is expressed as $r_0 = \dfrac{\Gamma^2}{1-\Gamma} r_{\rm g}$, where Γ is the central luminosity normalized by the Eddington luminosity and $r_{\rm g}$ is the Schwarzschild radius of the central object. As a result, the nearly Keplerian rotating disk outside r_0 turns to a nearly radial flow inside r_0. Furthermore, in the vicinity of the central object the infall velocity attains a terminal value, at which the effective gravity is balanced by radiation drag. The terminal speed v_∞ is found to be $v_\infty = -\dfrac{1-\Gamma}{2\Gamma} c$. Such accretion disks, where the angular momentum is removed via the external drag of radiation fields from the central source, are possible in several astrophysical contexts. For example, in the case of an X-ray burster the radiation density at the burst phases is very high in the inner region of the accretion disk, and therefore, the gas-accretion processes are remarkably enhanced due to the external radiation drag. Also, in a protoplanetary disk the external radiation drag may play an important role if a sufficient amount of dust exists in the disk.

Key words: Accretion disks — Active galactic nuclei — Protoplanetary disks — Radiation drag — X-rays: binaries

1. Introduction

In a wide range of astrophysical contexts, an accretion disk is commonly believed to be a prime-mover of various active phenomena. In star-forming regions, accretion disks are formed around a protostar, drive (or at least assist) bipolar jets, and eventually evolve to protoplanetary disks. In a close binary system, such as cataclysmic variables and X-ray binaries, an accretion disk, which is formed around a compact star due to gas supply from a companion, is responsible for such violent events as novae and X-ray bursters, and shines brighter than the stars. Also, the peculiar galactic object SS 433 exhibits a pair of subluminal jets which are ejected from a geometrically thick disk formed around a compact object. Finally, accretion disks in active galactic nuclei are believed to work as a central engine of the activity and to produce extragalactic radio jets.

In the current picture of an accretion disk, the angular momentum of the disk gas is transferred outward via *internal viscosity*, which originates from turbulent/magnetic motions, and consequently, the gas accretes onto the center (Shakura, Sunyaev 1973). This model is referred to as the standard model or the α-viscosity model. Very recently, a new mechanism by which angular momentum is removed via *radiation drag* due to the cosmological background radiation fields during the early universe has been proposed and investigated to some extent (Loeb 1993; Umemura et al. 1993). Based

on this mechanism, *cosmological accretion disks* (β-disk), in which the angular momentum is removed via *external radiation drag*, have been investigated by Fukue and Umemura (1994) and Tsuribe et al. (1994) (see also Umemura, Fukue 1994 for a spherical case).

In accretion disks around neutron stars, on the other hand, the importance of radiation drag was also pointed out (Fortner et al. 1989; Lamb 1989, 1991; Miller, Lamb 1993). That is, they discussed the idea that radiation drag causes the plasma in the inner corona near to the neutron star to lose its angular and vertical momenta and to fall approximately radially toward the star (Fortner et al. 1989; Lamb 1989, 1991). Along these lines, Fortner et al. (1989) carried out numerical simulations of radial accretion flow near to the neutron stars under a radiation force, using a one-dimensional, time-dependent radiation hydro-code. Miller and Lamb (1993) computed the trajectories of test particles immersed in radiation fields emitted from a neutron-star surface. In these studies, however, they considered the particle dynamics; i.e., the effect of gas pressure, or further, the structure of the accretion disks was not examined.

The aim of this paper is thus to consider the properties of gaseous disks immersed in radiation fields from a central luminous source in the context of such a new mechanism of angular-momentum removal through the *external radiation drag*.

In the next section the basic equations are described. The accretion disks/disk accretions in a point-mass potential are presented in section 3. In section 4, the general consequences of such accretion under the external radiation drag are discussed. Some astrophysical applications of such accretion disks are also considered in section 4. The results are summarized in section 5.

2. Basic Equations

Let us suppose an axisymmetric gaseous disk which is steadily rotating around a central object of mass M. We ignore the self-gravity of the disk gas. The disk is assumed to be geometrically thin, and therefore, the physical quantities are integrated over the vertical direction. It is also assumed to be effectively optically thin. We use cylindrical coordinates (r, φ, z) with the z-axis along the rotation axis of the disk, and adopt the Newtonian formalism for simplicity. Under these assumptions the basic equations governing the structure of the disk immersed in radiation fields produced by the central luminous object are described as follows.

The continuity equation is

$$2\pi r \Sigma v_r = -\dot{M}, \tag{1}$$

where Σ is the surface density, v_r the radial infalling velocity, and $\dot{M}$ the constant accretion rate. Using the density ρ of the disk gas and the half-thickness H of the disk, the surface density is expressed as $\Sigma = 2\rho H$.

The equations for radiation hydrodynamics in a moving plasma are found in, e.g., Hsieh and Spiegel (1976) and Fukue et al. (1985). To the lowest order of $\boldsymbol{v}/c$, where $\boldsymbol{v}$ is the bulk velocity of the plasma and c the light speed, the equation of motion in the radial direction under the influence of radiation fields is

$$v_r \frac{dv_r}{dr} - \frac{v_\varphi^2}{r} = -\frac{1}{\Sigma}\frac{d\Pi}{dr} - \frac{GM}{r^2} + \frac{1}{\rho}\frac{n_e \sigma_T}{c}\left(F - v_j P^{ij} - E v_r\right), \tag{2}$$

where v_φ is the azimuthal rotation velocity, Π $(= 2pH)$ the gas pressure integrated over the vertical direction (p being the pressure of the disk gas), n_e the electron number density, σ_T the Thomson scattering cross section, E the radiation energy density, F the radiation flux, and P^{ij} the radiation stress tensor. The third term on the right-hand side of equation (2) is the radiation force and the radiation drag force, which is proportional to the velocity.

For a radiation field produced by a central source with luminosity L, the radiation flux F is expressed as $F = L/4\pi r^2$ and the radiation energy density E becomes F/c at large r. Furthermore, the rr- and $r\varphi$-components of the radiation stress tensor P^{ij} are given as $P^{rr} = E$ and $P^{r\varphi} = 0$, respectively. Hence, the equation of motion in the radial direction is rewritten as

$$v_r \frac{dv_r}{dr} - \frac{v_\varphi^2}{r} = -\frac{1}{\Sigma}\frac{d\Pi}{dr} - \frac{GM}{r^2}\left(1 - \Gamma + 2\Gamma\frac{v_r}{c}\right). \tag{3}$$

Here, we introduce the parameter Γ, which expresses the ratio of the radiation force to the gravitational force:

$$\Gamma = \chi_e \frac{L}{L_E}, \tag{4}$$

where $\chi_e (= n_e/n_p)$ is the ionization rate (n_p being the proton number density) and $L_E (= 4\pi c G M m_p/\sigma_T)$ is the Eddington luminosity (m_p being the proton mass). For fully ionized electron-proton plasmas, this parameter Γ is just the central luminosity normalized by the Eddington luminosity, and therefore, should be less than or equal to unity (for electron-positron plasmas Γ becomes of the order of m_p/m_e).

The equation of motion in the azimuthal direction under the influence of radiation fields is

$$v_r \frac{dv_\varphi}{dr} + \frac{v_r v_\varphi}{r} = -\frac{1}{\rho}\frac{n_e \sigma_T}{c}\left(v_j P^{ij} + E v_\varphi\right). \tag{5}$$

Here, the right-hand side comes from the external radiation drag, which plays an essential role in the present model. For the present case where the radiation field is produced by the central source, the $\varphi\varphi$-component of the radiation stress tensor P^{ij} vanishes ar large r. Hence, by using the parameter Γ, this equation (5) can also be rewritten as

$$v_r \frac{dv_\varphi}{dr} + \frac{v_r v_\varphi}{r} = -\frac{GM}{r^2}\Gamma\frac{v_\varphi}{c}. \tag{6}$$

The hydrostatic balance in the vertical direction is integrated as

$$\frac{\Pi}{\Sigma} = \frac{GM}{r^3}\frac{H^2}{2}, \tag{7}$$

which gives the half-thickness H of the disk.

Finally, the equation of state is

$$p = \frac{\mathcal{R}}{\mu}\rho T, \tag{8}$$

where $\mathcal{R}$ is the gas constant and μ the mean molecular weight. In the present paper we ignore the heating and/or cooling inside the disk; we assume, if necessary, that the disk gas is isothermal.

3. Accretion Disks Driven by External Radiation Drag

Now we examine an accretion disk/disk accretion, where the mass accretion is caused by *external radiation drag* instead of internal friction. In order to understand the basic properties of the present accretion problem, we first examine the cold case, where the pressure-gradient force is ignored, and then consider the transonic nature of the present flow.

3.1. Cold Regime

In the cold case, equations (3) and (6), which govern the dynamical properties of accretion, become respectively

$$v_r \frac{dv_r}{dr} = \frac{v_\varphi^2}{r} - \frac{GM}{r^2}\left(1 - \Gamma + 2\Gamma\frac{v_r}{c}\right), \tag{9}$$

$$\frac{v_r}{r}\frac{d}{dr}(rv_\varphi) = -\frac{GM}{r^2}\Gamma\frac{v_\varphi}{c}. \tag{10}$$

When there is no radiation field ($\Gamma = 0$), this is the familiar infall problem with constant specific angular momentum. That is, it is well known that above equations (9) and (10) have an *infalling type solution*, where $v_r = -\sqrt{2E + 2GM/r - J^2/r^2}$ and $v_\varphi = J/r$, E (specific energy) and J (specific angular momentum) being constant. This infalling solution, however, has an infinite angular-momentum barrier near to the center. Hence, no accretion takes place for $\Gamma = 0$ under the Newtonian approximation. [It should be noted that in the relativistic case accretion is possible, since the height of the angular-momentum barrier becomes finite (see Fukue 1987 and references therein).]

On the other hand, when there is an interaction between the disk gas and radiation fields ($\Gamma \neq 0$), the angular momentum is removed and accretion may become possible even in the Newtonian case (cf. Fukue, Umemura 1994 for cosmological accretion disks).

Before discussing the numerical solutions of equations (9) and (10), we examine the asymptotic behavior of these equations. That is, near to the center we expand v_r and v_φ, substitute them into equations (9) and (10), and then collect the leading terms. Consequently, as the only physically meaningful solutions, we find the asymptotic solutions near to the center such as

$$v_r = v_\infty, \tag{11}$$

$$v_\varphi \propto \frac{1}{r}e^{-r_0/r}. \tag{12}$$

Here, the characteristic velocity v_∞ is

$$v_\infty = -\frac{1-\Gamma}{2\Gamma}c. \tag{13}$$

That is, the infall velocity reaches this *terminal speed* v_∞ when the effective force is balanced by radiation drag. The characteristic radius r_0 is expressed as

$$r_0 = \frac{GM(1-\Gamma)}{2v_\infty^2} = \frac{\Gamma^2}{1-\Gamma}r_g, \tag{14}$$

where $r_g = 2GM/c^2$ is the Schwarzschild radius of the central object. Inside this characteristic radius r_0 the angular momentum is quickly lost and the rotating flow turns to radially infalling flow. Considering the fact that the infall velocity cannot exceed c, we find that the condition that $\Gamma > 1/3$ should be satisfied for the gas to accrete onto the center under the present Newtonian approximation.

Far from the center, similar procedures yield the following asymptotic solutions at infinity:

$$v_r = -\frac{GM(1-\Gamma)}{|v_\infty|}\frac{1}{r} = -\frac{2GM\Gamma}{cr}, \tag{15}$$

$$v_\varphi = \sqrt{\frac{GM(1-\Gamma)}{r}}. \tag{16}$$

In the intermediate region of r, we should solve equations (9) and (10) numerically. In figure 1 we show the numerical solution which satisfies boundary conditions (11) and (12) near to the center and (15) and (16) at infinity. In figure 1 the abscissa is the radius r in units of r_0 and the ordinate is the velocity in units of v_∞.

As a result, due to the existence of external drag, disk accretion to the central object takes place in the cold case.

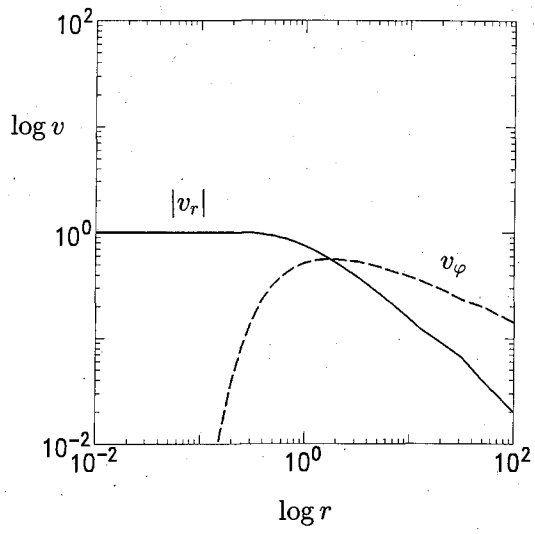

Fig. 1. Examples of numerical solutions in the cold regime. The abscissa is the radius r in units of r_0 and the ordinate is the velocity in units of v_∞. A solid curve denotes the infall velocity v_r while a dashed curve represents the rotating velocity v_φ.

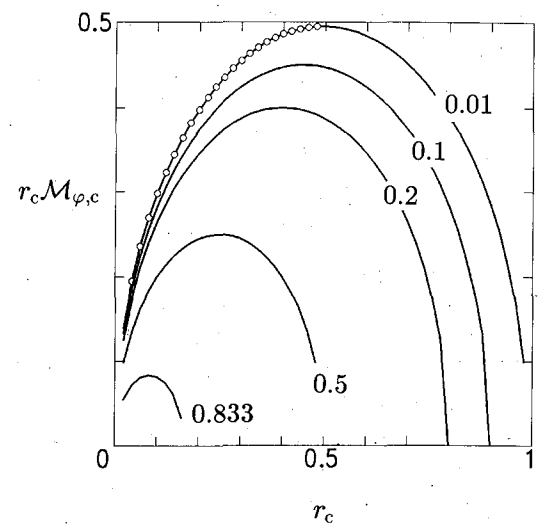

Fig. 2. Critical curves on the sonic plane ($\mathcal{M}_r = -1$) for the warm-isothermal accretion for several values of $\tilde{\beta}(= c_s/|v_\infty|)$. The abscissa is the critical radius r_c while the ordinate is $r_c\mathcal{M}_{\varphi,c}$. Solid curves represent the saddle type whereas small circles denote the center type.

3.2. *Warm Regime*

Here, let us examine the effect of pressure on the present accreting flow. In such a warm case the problem is reduced to transonic accretion flow onto the central object with external drag. Since the essential properties are the same between the adiabatic and isothermal cases, for simplicity we assume that the flow is *isothermal*: $\Pi/\Sigma = c_s^2$ (c_s being a constant isothermal sound speed).

Then, after some manipulations the basic equations (1), (3), and (6) are rearranged to

$$\frac{dv_r}{dr} = \frac{v_r\left[\dfrac{v_\varphi^2}{r} + \dfrac{c_s^2}{r} - \dfrac{GM(1-\Gamma)}{r^2}\left(1 - \dfrac{v_r}{v_\infty}\right)\right]}{v_r^2 - c_s^2}, \tag{17}$$

$$\frac{dv_\varphi}{dr} = -\frac{v_\varphi}{r} + \frac{GM(1-\Gamma)}{2r^2}\frac{v_\varphi}{v_\infty v_r}. \tag{18}$$

Introducing the radial Mach number, $\mathcal{M}_r$ ($= v_r/c_s$), and azimuthal Mach number, $\mathcal{M}_\varphi$ ($= v_\varphi/c_s$), and measuring the radius in units of $GM(1-\Gamma)/c_s^2$, we rewrite the above equations (17) and (18) as

$$\frac{d\mathcal{M}_r}{dr} = \frac{\mathcal{M}_r\left[\dfrac{\mathcal{M}_\varphi^2}{r} + \dfrac{1}{r} - \dfrac{1}{r^2}\left(1 + \tilde{\beta}\mathcal{M}_r\right)\right]}{\mathcal{M}_r^2 - 1}, \tag{19}$$

$$\frac{d\mathcal{M}_\varphi}{dr} = -\frac{\mathcal{M}_\varphi}{r} - \frac{\tilde{\beta}}{2r^2}\frac{\mathcal{M}_\varphi}{\mathcal{M}_r}, \tag{20}$$

where the only parameter $\tilde{\beta}$ is defined as

$$\frac{1}{\tilde{\beta}} = \left|\frac{v_\infty}{c_s}\right| = \frac{1-\Gamma}{2\Gamma}\frac{c}{c_s}. \tag{21}$$

As is easily expected, the physical meaning of $\tilde{\beta}$ is just the reciprocal of the radial Mach number near to the center. These equations are the so-called *wind equations* for the present problem.

When there is no external drag ($\tilde{\beta} = 0$), these equations are reduced to those for well-known disk accretion onto a central object with constant specific angular momentum (e.g., Limber 1967; Henriksen, Heaton 1975; Liang, Thompson 1980; Fukue 1987 and references therein). Transonic accretion under the *external radiation drag*, such as in the present problem, however, has not been investigated, except for the cosmological accretion disk (Fukue, Umemura 1994; Tsuribe et al. 1994; Takahashi et al. 1994).

3.2.1. *Critical curves and topologies*

As is well known, wind equations (19) and (20) become critical/transonic at the radius where the denominator and numerator vanish simultaneously. When there is no drag ($\tilde{\beta} = 0$), we have two critical points: one is a saddle (solar wind type), where the transonic flow passes through and the other is a center, where the flow cannot pass (e.g., Henriksen, Heaton 1975). In the present case, we have not critical points but *critical curves*; equations (19) and (20) are critical not at some points but on a

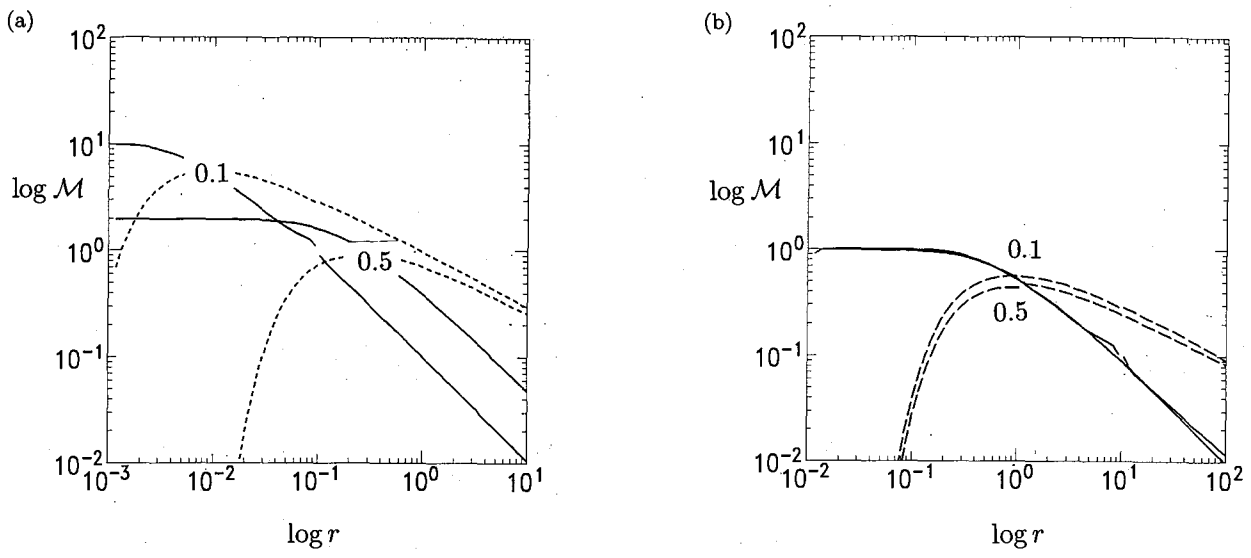

Fig. 3. Examples of transonic solutions which satisfy the appropriate boundary conditions. (a) The abscissa is the radius r in units of $GM(1-\Gamma)/c_s^2$ while the ordinate is the radial Mach number v_r/c_s (solid curves) and the azimuthal Mach number v_φ/c_s (dashed curves). The value of $\tilde{\beta}$ is for $\beta = 0.1$ and 0.5. The physical quantities at the critical points for these examples are $r_c = 0.0995$ and $\mathcal{M}_{\varphi,c} = 2.836$ for $\tilde{\beta} = 0.1$ and $r_c = 0.275$ and $\mathcal{M}_{\varphi,c} = 0.905$ for $\tilde{\beta} = 0.5$. (b) The same solutions, but the radius is in units of the characteristic radius r_0 and the ordinate is the velocities in units of the terminal speed v_∞.

curve in the $(r, \mathcal{M}_r, \mathcal{M}_\varphi)$-phase space, since the specific angular momentum is no longer conserved.

The critical conditions for accretion ($\mathcal{M}_r < 0$) are

$$\mathcal{M}_{r,c} = -1, \tag{22}$$

$$\mathcal{M}_{\varphi,c}^2 = -1 + (1-\tilde{\beta})/r_c, \tag{23}$$

where the subscript c denotes "critical". Equations (22) and (23) determine the *critical curve* in the $(r, \mathcal{M}_r, \mathcal{M}_\varphi)$-phase space for each value of $\tilde{\beta}$. The flow is also *transonic* on this curve in the sense that the radial Mach number is -1 there.

The loci and types of critical curves on the sonic plane ($\mathcal{M}_r = -1$) are shown in figure 2 for several values of $\tilde{\beta}$. In figure 2 the abscissa is the critical radius r_c while the ordinate is $r_c\mathcal{M}_{\varphi,c}$ there. Solid curves represent the saddle type, whereas the small circles denote the center type. In order for a positive r_c to exist, $\tilde{\beta}$ must be less than unity; i.e., the terminal radial Mach number v_∞/c_s is less than -1.

3.2.2. *Critical solutions*

For a given $\tilde{\beta}$ there are many transonic solutions which cross the critical curve at one point of the saddle type, according to various boundary conditions. We must therefore specify the appropriate boundary condition for the present problem. Similar to the cold case, we expand variables $\mathcal{M}_r$ and $\mathcal{M}_\varphi$ near to the center and far from the center, and obtain the asymptotic solutions. Near to the center the only asymptotic solutions which are physically meaningful are

$$\mathcal{M}_r = -\frac{1}{\tilde{\beta}} \quad (r \to 0), \tag{24}$$

$$r\mathcal{M}_\varphi \propto \exp\left(-\frac{\tilde{\beta}^2}{2r}\right) \quad (r \to 0). \tag{25}$$

These are just the same as the asymptotic solutions (12) and (13) for the cold case. That is, near to the center the angular momentum drops exponentially and the radial Mach number becomes a constant terminal one v_∞/c_s. Indeed, all of the transonic solutions for some $\tilde{\beta}$ approach these asymptotic solutions near to the center, although this is not the case far from the center.

Far from the center, on the other hand, the appropriate asymptotic solutions are

$$\mathcal{M}_r = -\frac{\tilde{\beta}}{r} \quad (r \to \infty), \tag{26}$$

$$\mathcal{M}_\varphi = \frac{1}{\sqrt{r}} \quad (r \to \infty). \tag{27}$$

That is, the flow must be Keplerian at infinity.

An example of transonic solutions which satisfies the above boundary conditions is shown in figure 3. In figure 3a the abscissa is the radius r in units of $GM(1-\Gamma)/c_s^2$ while the ordinate is the Mach numbers. The parameter $\tilde{\beta}$ is $\tilde{\beta} = 0.1$ and 0.5; i.e., the terminal radial

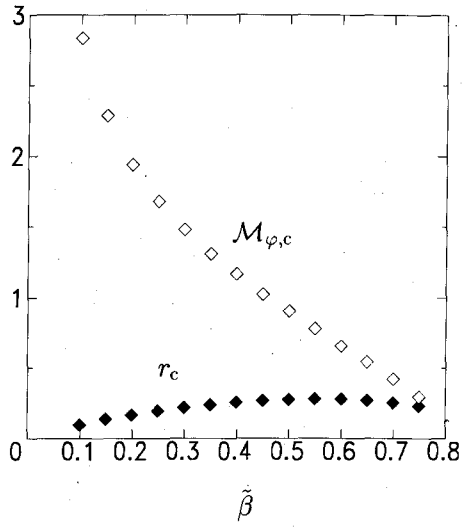

Fig. 4. Physical quantities at the critical points for transonic solutions satisfying the appropriate boundary conditions as a function of $\tilde{\beta}$.

Mach number is 10 and 2. The physical quantities at the critical point for these examples are $r_c = 0.0995$ and $\mathcal{M}_{\varphi,c} = 2.836$ for $\tilde{\beta} = 0.1$ and $r_c = 0.275$ and $\mathcal{M}_{\varphi,c} = 0.905$ for $\tilde{\beta} = 0.5$. In order to compare this warm case with the previous cold case, the same solutions are displayed in figure 3b, where the radius is in units of the characteristic radius r_0 and the ordinate is the velocities in units of the terminal speed v_∞.

In the warm case, losing angular momentum through the action of external drag, the flow initially accretes with almost Keplerian, passes through the transonic point, and then quickly loses angular momentum to infall almost radially until the effective gravity is balanced by radiation drag.

In figure 4 we summarize the physical quantities at transonic points as a function of $\tilde{\beta}$. The fact that r_c slowly increases and $\mathcal{M}_{\varphi,c}$ decreases with respect to $\tilde{\beta}$ is physically interpreted as follows. In the present case where external radiation drag is caused by radiation fields of the central luminous source, radiation drag is effective near to the center. If $\tilde{\beta}$ becomes larger, the characteristic radius r_0 (14), and therefore the radially infalling region, extends outwards, so that the sonic point moves gradually outwards. Since the angular momentum is also lost in the outer region, $\mathcal{M}_\varphi$ at the critical points decreases as $\tilde{\beta}$ increases. In these solutions the types of critical points are always saddles.

It should be noted that there exists a restriction on the range of $\tilde{\beta}$: $0.1 \leq \tilde{\beta} \leq 1$. For small $\tilde{\beta}$ (≤ 0.1), the type of critical point becomes center and the solution cannot pass there (see figure 2). For large $\tilde{\beta}$ (≥ 1), on the other hand, the drag is so strong that the azimuthal Mach number vanishes [see the critical condition (23)].

4. Discussion

4.1. General Properties

Similar to cosmological accretion disks, where the gas interacts with the cosmic background radiation (Fukue, Umemura 1994), in the present disk, which is immersed in external radiation fields around the central source, the disk gas can accrete steadily due to the angular-momentum removal via radiation drag. We call this type of accretion disk the *β-disk*. However, there exist several distinct properties between the cosmological accretion disks and the present disks, since the radiation-drag coefficient is spatially constant in the former, but in the present case it is inversely proportional to r^2.

For example, when the rotating velocity is written as a power of r (say, $v_\varphi \propto r^b$), from the angular momentum equation (6) the infalling velocity v_r *must* be proportional to $1/r$:

$$v_r = -\frac{GM\Gamma}{(b+1)c}\frac{1}{r}. \tag{28}$$

This is just the consequence of the fact that the radiation-drag coefficient is not constant but proportional to $1/r^2$. This power-law type solution is realized far from the center; equation (15). In the outer region the infall timescale $t_{\rm infall}$ is

$$t_{\rm infall} = \left|\frac{r}{v_r}\right| = \frac{(b+1)}{\Gamma}\frac{r^2}{r_g c}. \tag{29}$$

In cosmological accretion disks (Fukue, Umemura 1994), on the other hand, homologous accretion takes place when the rotating velocity is written as a power of r, since the infalling velocity is proportional to r and the infall timescale is uniform in such a region.

Otherwise, the angular-momentum equation (6) has an exponential-type solution; e.g., if v_r is constant,

$$rv_\varphi \propto \exp\left(\frac{GM\Gamma}{cv_r r}\right). \tag{30}$$

This is just the asymptotic solution (12) near to the center.

As a result, there appears the characteristic radius r_0 [equation (14)], inside which radiation drag of the central radiation fields is effective and rotating flow turns to radial flow with the terminal speed v_∞ [equation (13)], which the radial velocity approaches near to the center.

For *nearly* an Eddington limit case ($\Gamma \sim 1$), similar expressions were obtained by Lamb and colleagues (e.g., Fortner et al. 1989; Lamb 1989, 1991), although the factor is somewhat different from the present results. For example, they argued that inside the radius $r_{\rm radial} \sim 2\pi GM(1-\epsilon)^2/(\epsilon c^2)$, where their $1-\epsilon$ is equal

to the present Γ, radiation drag removes the angular and vertical momentum of the plasma in the disk corona (Lamb 1989, 1991). That is, their value for the characteristic radius is about 3.5 times larger than the present value. Moreover, they concluded that the radial velocity reaches the value $\epsilon c/2$ [$(1-\Gamma)c/2$ in the present notation] at which the comoving luminosity equals $L_{\rm E}$ and the acceleration vanishes (Miller 1990). This is also different from the present value by a factor of Γ. It should be noted that the present results are valid for general Γ and are consistent with their results when $\Gamma \sim 1$.

In order for the angular momentum of the gas to be removed effectively via the interaction between free electrons and photons, the gas should be optically thin. The radiation of the central source penetrates the disk gas from both the inner edge of the disk (toward the radial direction) and the surface of the disk (toward the vertical direction). The optical depth $\tau_{\rm ver}$ of the present disk in the vertical direction is, for the asymptotic solution far from the center,

$$\tau_{\rm ver} = \kappa\Sigma = \frac{(b+1)c\kappa\dot{M}}{2\pi GM\Gamma}, \tag{31}$$

where κ is the electron-scattering opacity and we used equations (1) and (28). Using the definition of parameter Γ and inserting the numerical values, we obtain the optical depth for the asymptotic solution far from the center:

$$\tau_{\rm ver} = 2.0\frac{(b+1)\kappa_{0.4}}{\chi_{\rm e}}\frac{\dot{M}c^2}{L}, \tag{32}$$

where $\kappa_{0.4} = \kappa/0.4\,{\rm cm^2\,g^{-1}}$. Thus, the optical depth far from the center is of the order of unity (furthermore, *constant*) as long as $L \sim \dot{M}c^2$.

On the other hand, the optical depth $\tau_{\rm rad}$ of the present disk in the radial direction is, for the asymptotic solution near to the center,

$$\begin{aligned}\tau_{\rm rad} &= \kappa\int_{r_{\rm in}}^{r}\rho dr \\ &= -\frac{\kappa\dot{M}}{4\pi v_\infty}\sqrt{\frac{GM}{2c_s^2}}\left(\frac{2}{3}r_{\rm in}^{-3/2} - \frac{2}{3}r^{-3/2}\right),\end{aligned} \tag{33}$$

where $r_{\rm in}$ is the inner radius of the disk and we used equations (1) and (7). Using the definition of v_∞, we obtain the optical depth in the radial direction as

$$\tau_{\rm rad} = \frac{2}{3}\frac{\Gamma}{1-\Gamma}\frac{c}{c_s}\frac{\dot{M}c^2}{L_{\rm E}}\left[\left(\frac{r_{\rm in}}{r_{\rm g}}\right)^{-3/2} - \left(\frac{r}{r_{\rm g}}\right)^{-3/2}\right], \tag{34}$$

which depends especially on the radius r and sound speed c_s for $\Gamma \sim 1$ and $\dot{M}c^2 \sim L_{\rm E}$. In the inner disk ($r \sim r_{\rm in}$), however, $\tau_{\rm rad}$ is always less than unity, irrespective of the values of the parameters.

4.2. Astrophysical Applications

In several astrophysical situations, accretion disks/disk accretion where the angular momentum is removed via the external radiation drag may be realized. In this subsection we discuss accretion disks under external drag regarding several astrophysical aspects.

4.2.1. Accretion disks in X-ray bursters

Accretion disks which form around compact stars, such as neutron stars and white dwarfs in close binaries, play dominant roles there. Apart from the quiescent stage where the disk gas is irradiated by the central object (Fukue, Sanbuichi 1993), the intensity of radiation from the central object is remarkably enhanced during a nuclear explosion on its surface. Although in nova outbursts the accretion disk surrounding a white dwarf may be destroyed, in X-ray bursts only the innermost region of the disk around a neutron star may be destroyed (Fukue 1982, 1983). An accretion disk around a neutron star as well as its corona (Lamb 1991) is therefore subject to the influence of radiation drag, as considered here.

Let us suppose a gaseous disk exposed to an intense radiation field during X-ray bursts. The radiation energy density ε at a distance r from the central object with luminosity L and radius R is expressed as

$$\begin{aligned}\varepsilon &= \frac{4\pi I}{c}\frac{1}{2}\left[1-\sqrt{1-\left(\frac{R}{r}\right)^2}\right] \\ &= \frac{4}{c}\frac{L}{4\pi R^2}\frac{1}{2}\left[1-\sqrt{1-\left(\frac{R}{r}\right)^2}\right] \\ &= \frac{1}{c}\frac{L}{4\pi r^2} \quad (r \gg R),\end{aligned} \tag{35}$$

where I is the specific intensity of the central object, which is assumed to be isotropic. When the luminosity of the central object is set to be the Eddington luminosity, $L_{\rm E}$ ($= 4\pi cGMm_{\rm p}/\sigma_{\rm T}$), where M is the mass of the central object, then the proportional coefficient of external radiation drag in this case becomes

$$\begin{aligned}\beta &= \frac{4\sigma_{\rm T}\varepsilon\chi_{\rm e}}{3m_{\rm p}c} \\ &= \frac{c^3\Gamma}{3GM}\left(\frac{r}{r_{\rm g}}\right)^{-2} \\ &= 6.78\times10^4\Gamma\left(\frac{M}{M_\odot}\right)^{-1}\left(\frac{r}{r_{\rm g}}\right)^{-2}{\rm s^{-1}},\end{aligned} \tag{36}$$

where $r_{\rm g}$ ($= 2GM/c^2$) is the Schwarzschild radius of the central object. The non-dimensional β normalized by the angular speed, Ω ($= \sqrt{GM/r^3}$), is then

$$\frac{\beta}{\Omega} = \frac{2\sqrt{2}}{3}\Gamma\sqrt{\frac{r_{\rm g}}{r}}. \tag{37}$$

This implies that radiation drag is significant in the central region of $r \lesssim 100 r_{\rm g}$.

4.2.2. Proto-quasars

In cosmological accretion disks, where the angular momentum is removed via the uniform cosmic background radiation, the timescale of the drag is

$$t_{\rm cos} = 1.64 \times 10^5 \mu \chi_{\rm e}^{-1} \left(\frac{T_0}{2.74\,{\rm K}} \right)^{-4} \left(\frac{1+z}{400} \right)^{-4} {\rm yr}, \tag{38}$$

where T_0 is the present temperature of the cosmic background radiation (Fukue, Umemura 1994). Hence, at a redshift of several hundreds the disk gas can accrete via Compton drag momentum removal. However, once a central active nucleus (*a proto-quasar*) forms, the drag by the radiation from the central source may effectively remove the angular momentum, even at relatively low redshifts, via the mechanism shown in this paper, because the timescale is, from equation (36),

$$t_{\rm drag} = \frac{1}{\beta} = 4.7 \times 10^5 \, \Gamma^{-1} \left(\frac{M}{10^8 M_\odot} \right) \left(\frac{r}{10^5 r_{\rm g}} \right)^2 {\rm yr}, \tag{39}$$

which is significantly less than the Hubble expansion timescale at $z < 400$ for inner disk regions of $r < 10^5 r_{\rm g}$ [$\sim 1\ {\rm pc}\,(M/10^8 M_\odot)$]. Furthermore, it is worth noting that (39) is also smaller than the timescale of the α-viscosity:

$$t_{\rm vis} = 2.4 \times 10^7 \left(\frac{\alpha}{0.1} \right)^{-1} \left(\frac{M}{10^8 M_\odot} \right)^{1/2} \times \left(\frac{r}{10^5 r_{\rm g}} \right)^{1/2} \left(\frac{T}{10^4\,{\rm K}} \right)^{-1} {\rm yr}. \tag{40}$$

Thus, radiation drag may be the most dominant mechanism to remove angular momentum in proto-quasars, if the central luminous sources emit the radiation with nearly the Eddington luminosity.

4.2.3. Protoplanetary disks around a protostar

In protoplanetary disks which form around a newly born protostar the temperature of the disk gas is so low that the gas in the disk must be in neutral or in molecular states. Therefore, radiation drag between free electrons and photons does not work. However, submicron particles — *dust* — as well as free electrons are also subject to the influence of radiation fields. This is well-known as the *Poynting-Robertson effect* in the astrophysics of the Solar System.

Let us consider a solid particle — dust — moving in a circular orbit around the protostar. If the protoplanetary disks are optically thin to the appropriate range of electromagnetic radiation, the dust particle will constantly absorb photons through its isolated hemisphere and will radiate an equal amount of energy in the form of infrared radiation, which is emitted in all directions. Although the incident radiation has no angular momentum, the radiation emitted by the dust inherits its angular momentum. As a result, the angular momentum of the dust is carried out. This is the Poynting-Robertson effect (Poynting 1903; Robertson 1937).

Similar to the case of X-ray bursters, the radiative flux f at a distance r from the center is $f = L/4\pi r^2$, where L is the luminosity of the protostar. Since the radiation force (in unit mass) on the spherical particle with mass $m_{\rm d}$ and radius $a_{\rm d}$ is $\pi a_{\rm d}^2 f_r/(m_{\rm d} c)$, and therefore, radiation drag is $\pi a_{\rm d}^2 f/(m_{\rm d} c) \times (v/c)$, the proportional "coefficient" β is expressed as

$$\begin{aligned} \beta &= \frac{\pi a_{\rm d}^2 f}{m_{\rm d} c^2} \\ &= \frac{3L}{16\pi a_{\rm d} \rho_{\rm d} c^2 r^2} \\ &= 1.43 \times 10^{-11} \left(\frac{L}{L_\odot} \right) \left(\frac{a_{\rm d}}{10^{-4}\,{\rm cm}} \right)^{-1} \\ &\quad \times \left(\frac{\rho_{\rm d}}{2.5\,{\rm g\,cm^{-3}}} \right)^{-1} \left(\frac{r}{\rm AU} \right)^{-2} {\rm s}^{-1}, \end{aligned} \tag{41}$$

where $\rho_{\rm d}$ is the density of dust particles (Robertson 1937). The corresponding timescale (a few thousand years at 1 AU) is rather short. Hence, for the dust component in protoplanetary disks around a protostar the accretion process can be driven by the external radiation drag.

5. Conclusions

In this paper we considered accretion disks/disk accretions (the *β-disk*) where the angular momentum is removed not by the internal friction as standard α-disks but by the external radiation drag. We assume that external drag is proportional to the velocity and that the radiation field is exerted by the central luminous source.

Due to the effect of the external radiation drag, the angular momentum of gas is removed as in the case of the cosmological accretion disk discussed in a previous study (Fukue, Umemura 1994). In the present case, however, since the radiation energy density is inversely proportional to r^2, the angular momentum is quickly lost inside the characteristic radius r_0, which is expressed as $r_0 = \dfrac{\Gamma^2}{1-\Gamma} r_{\rm g}$, where Γ is the central luminosity normalized by the Eddington luminosity and $r_{\rm g}$ the Schwarzschild radius of the central object. Hence, the nearly Keplerian rotating disk outside r_0 turns to the nearly radial flow inside r_0. Furthermore, in the vicinity

of the central object the infall velocity attains the terminal one v_∞, which is expressed as $v_\infty = -\dfrac{1-\Gamma}{2\Gamma}c$, when the effective gravity is balanced by radiation drag.

In the cold regime, where the pressure gradient force is ignored, we found steady solutions such that the infalling velocity v_r is expressed as $v_r = -[GM(1-\Gamma)/|v_\infty|]/r$ far from the center and as $v_r = v_\infty = -\dfrac{1-\Gamma}{2\Gamma}c$ near to the center, while the rotation velocity v_φ is Keplerian far from the center (i.e., $v_\varphi = \sqrt{GM(1-\Gamma)/r}$) and exponentially drops near to the center (i.e., $v_\varphi \propto e^{-r_0/r}/r$). In the warm regime, where the effect of the gas pressure is taken into account, we found steady transonic solutions, such that the flow is initially accreting subsonically and rotating Keplerian far from the center, passes a sonic point, and eventually becomes almost radially accreting supersonic flow with no angular momentum.

These accretion disks where the angular momentum is removed via the external radiation drag by the central luminous source are possible in several astrophysical contexts, such as accretion disks around compact stars, proto-quasars, and dusty disks around protostars.

In the present analysis we simplified several situations. For example, we approximated the radiation energy density, assuming that the radius of the central object is sufficiently small. In general, as expressed in equation (35), there exists the dilution factor, which becomes important in the vicinity of the central object. Moreover, we adopted the Newtonian formalism, while the relativistic effect becomes important if the central object is a neutron star. These boundary effects, as well as the time-dependent behavior, should be taken into considerations in the future.

The authors would like to thank Professor S. Kato and Drs N. Shibazaki and S. Mineshige for valuable discussions. This work is supported in part by the Grant-in-Aid for Scientific Research by the Ministry of Education, Science and Culture of Japan (05640313 and 05854011).

References

Fortner B. A., Lamb F. K., Miller G. S. 1989, Nature 342, 775
Fukue J. 1982, PASJ 34, 483
Fukue J. 1983, PASJ 35, 355
Fukue J. 1987, PASJ 39, 309
Fukue J., Kato S., Matsumoto R. 1985, PASJ 37, 383
Fukue J., Sanbuichi K. 1993, PASJ 45, 831
Fukue J., Umemura M. 1994, PASJ 46, 87
Henriksen R. N., Heaton K. C. 1975, MNRAS 171, 27
Hsieh S.-H., Spiegel E. A. 1976, ApJ 207, 244
Lamb F. K. 1989, in Proc. 23rd ESLAB Symposium, ed J. Hunt, B. Battrick (ESA, Paris) vol 1, p215
Lamb F. K. 1991, in Neutron Stars: Theory and Observations, ed J. Ventura, D. Pines (Kluwer Academic Publishers, Dordrecht) p.445
Liang E. P. T., Thompson K. A. 1980, ApJ 240, 271
Limber D. N. 1967, ApJ 148, 141
Loeb A. 1993, ApJ 403, 542
Miller G. S. 1990, ApJ 356, 572
Miller G. S., Lamb, F. K. 1993, ApJL 414, L43
Poynting J. H. 1903, Phil. Trans. Roy. Soc. London, Ser. A, 202, 525
Robertson H. P. 1937, MNRAS 97, 423
Shakura N. I., Sunyaev R. A. 1973, A&A 24, 337
Takahashi A., Fukue J., Sanbuichi K., Umemura M. 1995, PASJ 47, 425
Tsuribe T., Umemura M., Fukue J. 1994, PASJ 46, 597
Umemura M., Fukue J. 1994, PASJ 46, 567
Umemura M., Loeb A., Turner E.L. 1993, ApJ 419, 459